Membrane parameters, signal transmission, and the design of a graded potential neuron

Hateren, J.H. van; Laughlin, S.B.

Published in:
Journal of comparative physiology a-Neuroethology sensory neural and behavioral physiology

Publication date:
1990

J Comp Physiol A (1990) 166:437–448

Journal of Comparative Physiology A Sensory, Neural, and Behavioral Physiology

Membrane parameters, signal transmission, and the design of a graded potential neuron

J.H. van Hateren[1] and S.B. Laughlin[2]

[1] Department of Biophysics, Groningen University, Westersingel 34, NL-9718 CM Groningen, The Netherlands
[2] Department of Zoology, Cambridge University, Downing Street, Cambridge CB2 3EJ, United Kingdom

Accepted September 29, 1989

Summary. 1. The large monopolar cells (LMCs) of the fly, *Calliphora vicina*, visual system transmit graded potentials over distances of up to 1.0 mm. An electrical model was constructed to investigate the design principles relating their membrane parameters to signal transmission and filtering.

2. Using existing anatomical measurements, a cable model (van Hateren 1986) was fitted to the measured intracellular responses of the cells to injected current. The LMC has three functional components: a distal synaptic zone of low impedance, an axon with high specific membrane resistance ($>50 \cdot 10^5$ M$\Omega \cdot \mu m^2$), and a high impedance proximal terminal. These components interact to transmit information efficiently. The low input impedance synaptic zone charges and discharges the axon rapidly, ensuring a good frequency response. The high resistance axon conducts signals with little decrement. The model shows that graded potential transmission in LMCs selectively filters synaptic noise and predicts the changes in response waveform that occur during transmission.

3. The parameters of the model were adjusted to determine the relative costs and benefits of alternative cable designs. The design used in LMCs is the most expensive and the most effective. It requires the largest currents to generate responses but transmits signals with least decrement. Parallel neurons in the fly visual system have fewer input synapses and this could low-pass filter their graded response.

Key words: Vision – Signal transmission – Graded potential

Introduction

The shape of a neuron and regional specializations of its membrane determine information processing and transmission. The Large Monopolar Cells (LMCs) of the fly visual system offer an opportunity to study the relationship between a neuron's structure and its function. This opportunity arises because, for LMCs, both the morphology and coding are relatively simple and have been described in some detail (revs. Shaw 1984; Laughlin 1987).

LMCs are essentially cylinders of 2–3 μm diameter and 250–1000 μm length. In the two largest and most commonly recorded LMCs, L1 and L2, the distal 50 μm receives an array of 1200 chemical synapses from a group of six photoreceptors (Nicol and Meinertzhagen 1982). The function of the LMC is to sum the photoreceptors' synaptic input in the synaptic zone (e.g. van Hateren 1987) and transmit the resulting graded potential several hundred μm to its proximal terminal. The synapses connecting the photoreceptors to an LMC are phasic in output (Järvilehto and Zettler 1971). Thus the LMC response codes changes in photoreceptor output over a wide range of illumination levels (Laughlin and Hardie 1978). The dynamics of the signal transmitted to LMCs is well documented (Laughlin et al. 1987). The relatively slow process of phototransduction low-pass filters the optical signal, generating very little signal power above 250 Hz. The photoreceptor synapses then amplify and high-pass filter this signal during transmission to LMCs. Thus the LMCs transmit a signal that is restricted to a well defined band of frequencies below 250 Hz. The LMC response is also contaminated with synaptic noise, much of it at higher frequencies than photoreceptor signals. Measurements of signal to noise ratios show that this noise could significantly impair visual acuity under daylight conditions (Laughlin et al. 1987).

Knowing the numbers and spatial distribution of photoreceptor synapses, and the dynamics of the signal and the noise, we can assess the role played by the LMC membrane in generating, filtering and transmitting the signal. We have measured the responses of LMCs to low density current pulses, injected into either the synaptic zone or the axon, and have used this data to revise a previous cable model of the LMC (van Hateren 1986). Our new model successfully predicts the changes in sig-

nal and noise levels that are brought about during passive signal propagation from the synaptic zone to the proximal terminal. We find that the cable properties of the LMC axon are matched to the dynamics of the signal so that it is transmitted with little decrement, and that synaptic noise is selectively attenuated. We conclude that the large number of synapses, and the resulting low input impedance of the synaptic zone, are essential for driving signals down the axon.

Methods

Electrophysiology. Female *Calliphora vicina* were prepared for intracellular recording from the lamina and first chiasm using standard procedures (Laughlin and Hardie 1978). All experiments were performed in darkness. Electrodes were either completely filled with a solution of 0.6 *M* potassium sulfate and 10 m*M* potassium chloride, or filled with 3.0 *M* potassium acetate in the tip and shank, and 3.0 *M* potassium chloride in the barrel. The electrodes selected had resistances of 70–100 MΩ and were connected to the headstage with a chloridized silver wire. The indifferent electrode was a fine chloridized silver wire, inserted in the opposite eye.

An Axoclamp-2A amplifier was operated in discontinuous current clamp mode to inject current and record responses. The switching rate was adjusted for each recording, in the range of 3.5–5.0 kHz, and the response of the headstage was continuously monitored throughout the experiment. With a driven shield and the point of insertion of the electrode sealed with silicon grease to prevent electrolyte creep, the time constant of capacity compensated electrodes was between 30 and 50 μs. This compares with a time constant of at least 0.5 ms for the lowest impedance region of the LMC. Under these conditions the switched clamp technique gives a reasonable approximation of the true LMC membrane potential produced by injected current (Laughlin and Osorio 1989). For each cell, the switched clamp recordings were checked by comparing them with responses to identical currents, injected using a balanced bridge circuit. In general, current pulses of less than 0.1 nA were injected to circumvent artifacts due to electrode polarization and the small (less than 10%) voltage sensitive effects found in LMCs (Laughlin and Osorio 1989). Records were averaged between 500 and 2000 times to improve accuracy. To control against changes in recording quality during averaging, the resting potential of the cell was continuously monitored and the cell input resistance and the amplitude of a saturated response to light were measured before and after averaging. With the exception of 2 cells in the chiasm, where recording conditions were more difficult, all cells generated hyperpolarizing responses of more than 30 mV.

The approximate recording position was established using physiological criteria (e.g. Laughlin and Osorio 1989). A recording site in the lamina is indicated by a depolarizing extracellular response to light, intracellular recordings from photoreceptor axon terminals in the immediate vicinity, and small changes in receptive field as one moves across the retinotopic array of cells. A site in the chiasm is indicated by large changes in the positions of receptive fields as one passes from cell to cell. The approximate position of the recording site along an axon in the chiasm was estimated from the electrode track and the position of the cell's receptive field (e.g. if the electrode is in the frontal region of the chiasm and the cell's receptive field originates in the lateral region of the retina, the axon must have crossed the midpoint of the chiasm and one is recording from the proximal third of a cell with a long axon). Recordings from ambiguous recording sites, close to the lamina, were rejected.

Modelling. Figure 1 summarizes some basics of cable modelling. Cables are characterized by distributed parameters: resistances and capacitances are not discrete components, but are distributed along the cable. This leads to the cable equation, a differential equation that can be readily solved for particular simple configurations (see e.g. Jack et al. 1975). More complicated configurations can be conveniently solved by computer, e.g. using a circuit analysis program, and to this end lumped circuit models are becoming increasingly popular. Figure 1 shows three such models.

The first lumped circuit model is just a simple *RC*-circuit, and assumes isopotentiality. This model is particularly suited for spherical cell bodies and rather short cable segments. The second model shown, also known as a compartmental model (see e.g. Segev et al. 1985), takes the intracellular resistivity into account, by adding a resistance to current flow along the cable. The membrane is still modelled as a single *RC*-circuit, and this assumes again isopotentiality. This model will work reasonably well for short cable segments and slowly varying voltages, but will break down for higher frequencies because the capacitance then forms a low-impedance pathway to ground which reduces isopotentiality – unless the cable segment is very short. The last model shown in Fig. 1 (see van Hateren 1986) considers the cable as a two-port, with independent voltages and currents at both terminals. The resulting t-circuit – which is not equivalent to the circuit of the compartmental model, and only coincidentally resembles it – is not an approximation, but gives a complete description of all voltages and currents in the cable segment. A disadvantage of this model is that it has no simple equivalent in the time-domain, which makes it difficult to implement nonlinear properties of the membrane. This is no drawback at all in the present study because, within their physiological range, LMC membranes are approximately linear (Wang-Bennett and Glantz 1987; Guy and Srinivasan 1988; Laughlin and Osorio 1989; Weckström et al. 1989).

Solutions to the equations describing a combination of cable segments (e.g. Fig. 2) were obtained in the frequency domain, using a ladder algorithm (see van Hateren 1986 for details). This problem lends itself to vectorization (where each voltage or current vector contains the voltages or currents for a suitable range of frequencies), and was implemented on an Analogic AP500 array processor connected to a Data General MV4000 minicomputer. The resulting speed of the calculations made it feasible to perform a least-squares fit to the data.

Details of the model and the procedure followed with the fitting can be found in Appendix A.

Results

Introduction

Before going into details of the models we used for the LMCs, we will first outline the structure of this type of neuron. An LMC can be divided into four components (Fig. 2A): the cell body, the synaptic zone in the lamina, the axon traversing the chiasm between lamina and medulla, and a terminal in the medulla (e.g. Guy and Srinivasan 1988). As far as we know the cell body has a very high resistance (R.C. Hardie, personal communication), does not receive synapses, and is not involved in signal generation. The synaptic zone in the lamina is a tube of 2–3 μm diameter with several hundred dendrites attached (Nicol and Meinertzhagen 1982). This zone receives the synaptic input from the photoreceptors. The resulting signal is transmitted along an axon of diameter 2–3 μm to the medulla. The axonal projection forms a chiasm, with anterior LMCs projecting to the lateral medulla and vice versa. Thus axon length varies with location, from approximately 250 μm to 1000 μm. Finally, the axon forms a terminal where synaptic input to medulla neurons is generated.

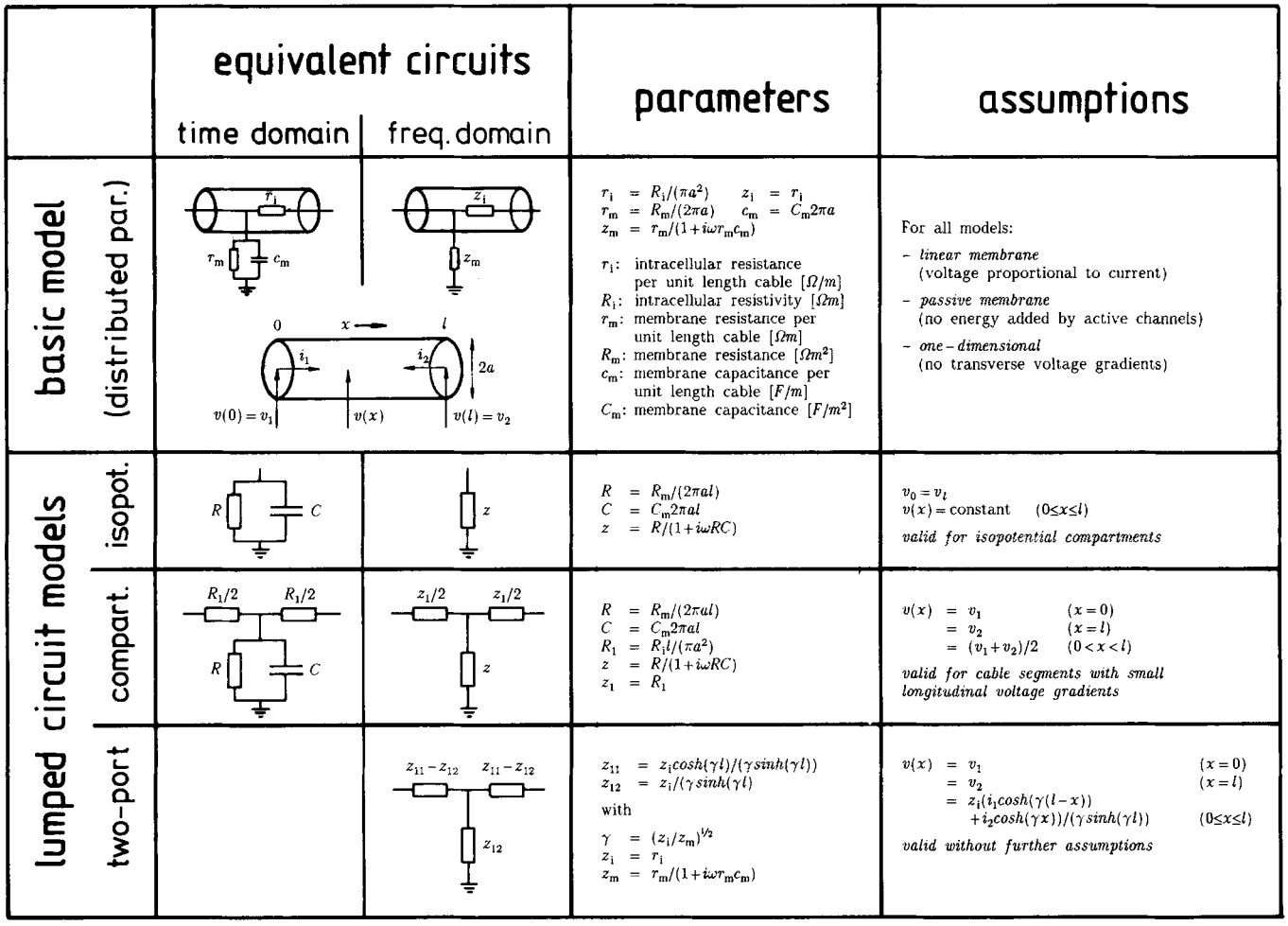

Fig. 1. Various models used in cable modelling. The basic model has distributed variables: the membrane has resistance and capacitance, the axoplasm resistance. A cable segment of length l and radius a can be considered as a two-port component, with voltage v_1 and current i_1 at the left terminal and v_2 and i_2 at the right one. Models shown are the isopotential model, compartmental model (see e.g. Segev et al. 1985), and two-port model (see van Hateren 1986)

The suitability of various models

The anatomy of the LMC (Fig. 2A) suggests that it should be modelled as 3 main components: 1) a synaptic zone with a large membrane area, 2) a long and slender axon, and 3) a terminal in the medulla. We found that it was not necessary to include the cell body. It could

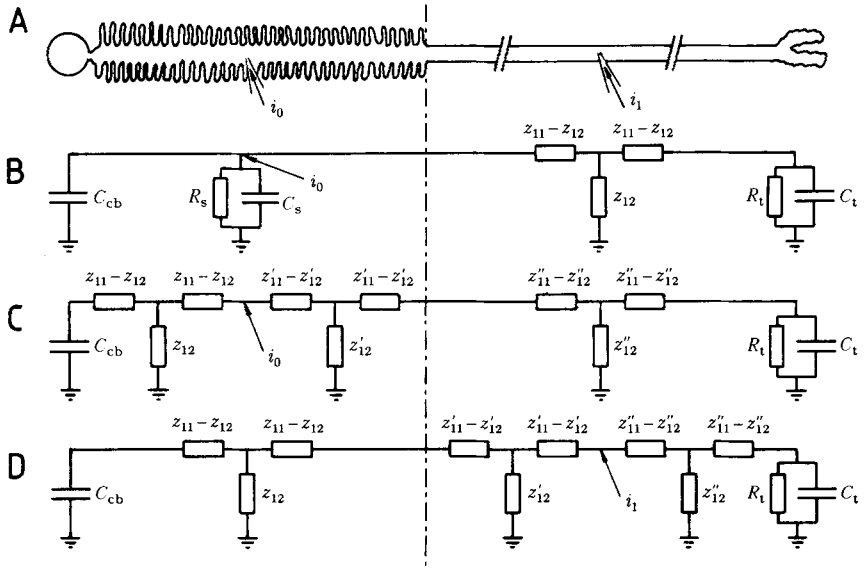

Fig. 2A. Schematic diagram of the anatomical layout of an LMC. From left to right we see the cell body; the synaptic zone in the lamina, the axon connecting lamina to medulla, and the terminal in the medulla. In experiments current could be injected either in the synaptic zone (i_0) or in the axon (i_1). **B.** Model with the synaptic zone considered as an *RC*-circuit. **C.** Model with the synaptic zone considered as two cable segments around the recording and current injecting electrode. **D.** Model used for measurements of responses to current injection in the axon

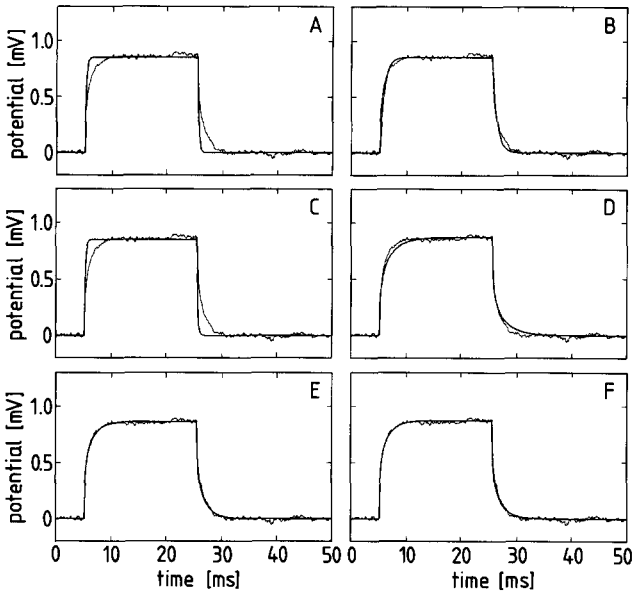

Fig. 3A–F. Six theoretical fits to an experimental charging curve ($i_{in}=0.05$ nA) showing the suitability of various models. **A.** Fit with an exponential (*RC*-circuit), with fixed S_{ms} (18 $\mu m^2/\mu m$) and R_{ts} as the only free parameter ($R_{ts}=17.0\,M\Omega$). **B.** Fit with an exponential with both S_{ms} and R_{ts} as free parameters ($S_{ms}=85$ $\mu m^2/\mu m$, $R_{ts}=17.1$ MΩ). **C.** Fit with a cable without a synaptic input segment, with fixed a_x (1.35 μm), and R_{mx} and l_x as free parameters ($R_{mx}=0.26\cdot10^5$ M$\Omega\cdot\mu m^2$, $l_x=500$ μm). **D.** Same as C, now with a_x, R_{mx}, and l_x as free parameters ($a_x=3.05$ μm, $R_{mx}=2.7\cdot10^5$ M$\Omega\cdot\mu m^2$, $l_x=1080$ μm). **E.** Fit with a cable and a synaptic input segment modelled as an *RC*-circuit, R_{mx} was found to be very large, and the fit further yielded $R_{ts}=17.4$ MΩ and $l_x=300$ μm. **F.** Fit with a cable and a synaptic input segment modelled as a short cable segment, R_{mx} was found to be very large, and $R_{ms}=0.224\cdot10^5$ M$\Omega\cdot\mu m^2$, $l_x=320$ μm. Other parameters (where applicable): $C_{cb}=260\cdot10^{-5}$ nF; $C_m=10^{-5}$ nF/μm^2; $R_i=0.8$ M$\Omega\cdot\mu m$; $R_{mx}=100\cdot10^5$ M$\Omega\cdot\mu m^2$; $a_x=1.35$ μm; $a_s=1.35$ μm; $l_s=50$ μm; $d_s=25$ μm; $R_{tt}=$ inf.; $S_{tt}=1000$ μm

be modelled as a single capacitance, but was found to have negligible influence on the behavior of the model. Furthermore, the dendrites of the synaptic zone need not be modelled separately because, as we show in Appendix B, the resistance of their stems usually makes a negligible contribution to the total input resistance of the synaptic zone (cf. Winslow et al. 1989). To demonstrate that all 3 components play an essential role in signal transmission we tested simpler models.

An example of a measurement we used for testing different models is shown in Fig. 3. We injected a current pulse into the synaptic zone of an LMC, while recording the intracellular potential by using a single-electrode current clamping device (see Methods). The voltage response to this current pulse is shown as the noisy trace of Fig. 3A–F. The smooth curves are fits to this data using various models of increasing complexity.

The simplest model was an *RC*-circuit, yielding an exponential charging curve. This model would be adequate if the LMC charging curve is dominated by the behavior of its synaptic membrane, i.e. if we assume a negligible influence of both the axon and the terminal. The total membrane area of the synaptic zone is estimated from published anatomical data (approximately 900 μm^2, see Appendix A), and this yields the capacitance C if we assume a standard value for the specific membrane capacitance $C_m=10^{-5}$ nF/μm^2 (1 $\mu F/cm^2$). R cannot be inferred from the membrane area because it depends on the exact value of the membrane resistance, which can be very different in different cells or parts of cells. Figure 3A shows the best theoretical fit (smooth curve) that could be obtained using R as a free parameter. In Fig. 3B both R and C were free parameters. The fit is better now, but from the C obtained from the fit one derives a synaptic membrane area of 4250 μm^2 – almost 5 times the anatomical estimate.

A second simple model assumes that the electrical properties of the synaptic zone and the axon are identical (e.g. Wang-Bennett and Glantz 1987). In this case the LMC can be modelled as a cable terminated with a terminal resistance (R_t) and a terminal capacitance (C_t). The entire LMC is equivalent to that part of the circuit in Fig. 2B which is to the right of the dashed line. We modelled this cable as a two-port t-circuit (lower panel of Fig. 1). Now there are more parameters involved: the diameter of the cable, its length, the specific membrane resistance of the axon, the terminal resistance, and the terminal capacitance. Of these only the length and the specific membrane resistance are unknown. The diameter of the cable is approximately 2.7 μm (Nicol and Meinertzhagen 1982), the terminal capacitance $1000\cdot10^{-5}$ nF (see Appendix A), and we assume a very large terminal resistance. This latter assumption is consistent with the small decrement of the signal as it travels along the axon (Zettler and Järvilehto 1973), and would, even if it is only approximately correct, barely influence the model calculations. Figure 3C shows the best fit that could be obtained using the length and specific membrane resistance of the axon as free parameters. In Fig. 3D the axon diameter was allowed to vary. The fit is now better than in Fig. 3C, but the length (1080 μm) and diameter (6.1 μm) of the axon obtained from the fit are incompatible with anatomical data. Though LMCs in particular parts of the eye have very long axons, the measurement of Fig. 3 was obtained from a part of the eye where the LMCs have axons of 250–400 μm. Clearly, a single homogenous cable cannot account for the electrical properties of an LMC.

Therefore, we finally modelled the LMC as shown in Fig. 2B and C. These two models take into account differences between the synaptic zone and the axon. Both models describe the data adequately (Fig. 3E and F, respectively). The difference between them is that Fig. 2B models the synaptic zone as an *RC*-circuit, and Fig. 2C as two small cable segments (one segment on either side of the electrode which is assumed to have impaled the synaptic cable segment at its midpoint). In both models the cell body is assumed to have negligible conductance, and a capacitance C_{cb} determined by its membrane area. In Fig. 3E the total resistance of the synapse, and the specific membrane resistance and length of the axon were treated as free variables. In Fig. 3F the specific membrane resistance of the synapse,

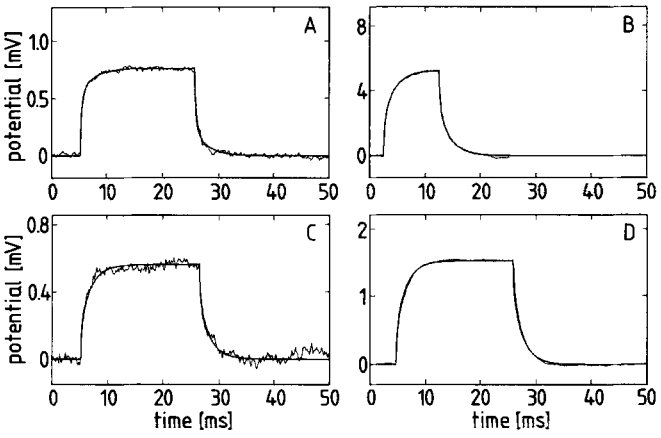

Fig. 4A–D. Examples of theoretical fits to experimental curves. **A.** Recording in the lamina, $i_{in}=0.05$ nA (parameters: $R_{ms}=0.196\cdot 10^5$ MΩ·μm^2, $l_x=440$ μm). **B.** Recording in the lamina, $i_{in}=0.5$ nA (parameters: $R_{ms}=0.202\cdot 10^5$ MΩ·μm^2, $l_x=380$ μm). **C.** Recording in the chiasm, $i_{in}=0.02$ nA (parameters: $l_x=350$ μm, $d_x=50$ μm). **D.** Recording in the chiasm, $i_{in}=0.05$ nA (parameters: $l_x=350$ μm, $d_x=70$ μm). Other parameters as in Fig. 3

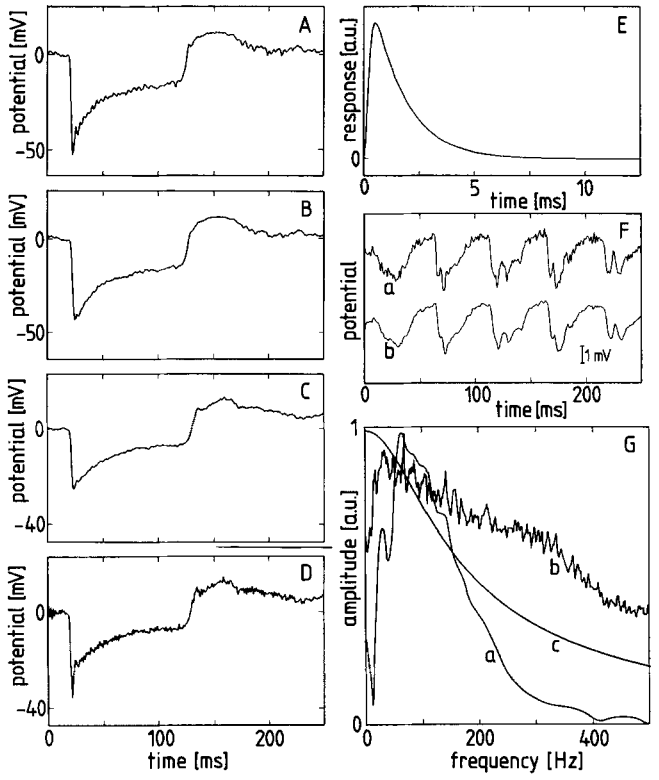

Fig. 5A–G. Evaluation of the cable model. **A.** Response recorded in the lamina to a light flash and **B**, the predicted response propagated to the medulla; parameters for the model as in the fit for Fig. 4A. **C.** Response recorded in the chiasm to a light flash. **D.** Prediction of the lamina response that generated the chiasm response; parameters as before. **E.** The impulse response for the voltage transfer of the cable as used in **B**. **F.** Upper trace: unaveraged response of an LMC in the lamina to a 20 Hz sine wave; lower trace: prediction by the model (parameters as in Fig. 4A) of how this response would look in the medulla. **G.** Transfer function of the cable (c) compared to the amplitude spectra of signal (a) and noise (b) as measured in a light-adapted LMC in the lamina

and the specific membrane resistance and length of the axon were free variables. Both fits yield realistic values of about 300 μm for the length of the axon. The fits are best if we assume a very high resistance of the axon membrane (larger than $50\cdot 10^5$ MΩ·μm^2) and a very high terminal resistance (see Appendix A).

Concluding, we see that simple models, like an *RC*-circuit or a single cable, yield either bad fits (Fig. 3A and C), or fair fits with unrealistic values for the parameters (Fig. 3B and D). Even these better fits are inferior to those obtained from the full model. Finally, we conclude that it makes virtually no difference whether the synaptic zone is modelled as a cable segment (Guy and Srinivasan 1988) or as an *RC*-circuit (van Hateren 1986). However, for current injection experiments the model using a cable segment (Fig. 2C) will give more realistic estimates of the specific synaptic membrane resistance, and is therefore used for that purpose. If we are interested, on the other hand, in the response of an LMC to a presynaptic voltage, the *RC*-model of the synaptic zone (Fig. 2B) is more realistic. This is because current is simultaneously injected through transmitter-driven channels distributed relatively uniformly along the synaptic zone, creating conditions that approximate isopotentiality more closely than when injecting current at one position through a microelectrode.

Two other examples of fits to experimental data obtained from current injection in the synaptic zone are shown in Fig. 4A and B. Figure 4C and D, on the other hand, are from current injection in the axon of the LMC in the chiasm. In the latter case we made fits using the model shown in Fig. 2D. The synaptic zone is one cable segment, and the axon consists of two more cable segments formed by the two parts of the axon distal and proximal to the recording electrode. The fits obtained to this kind of measurement were also satisfactory, and yielded lengths of the axon and positions of the electrode that were consistent with estimates following from the location of the recording. The results of 19 current injections in 15 cells were fitted by the model and yielded consistent estimates (Table 2 in Appendix A).

Predictions of the model

Some predictions of the model of Fig. 2B are shown in Fig. 5. In order to test the model we compared responses of LMCs to flashes of light, recorded either in the synaptic zone in the lamina or in the chiasm, close to the termination of the axon in the medulla. Figure 5A and C shows representative examples of light responses at these recording positions. The amplitudes of the responses differ somewhat from cell to cell, particularly in the chiasm, where recordings are less stable. Consequently, we will concentrate here on the shapes of the responses, which are quite consistent. The light responses in the axon generally show a less sharp peak

and a reduced noise level. We tested the model, using the parameters obtained from fits as in Figs. 3(E, F) and 4, by predicting the response one should observe at one position from the response recorded in another. Figure 5B is the LMC response in the chiasm that is predicted from the recording in the lamina of Fig. 5A, and Fig. 5D is the response in the lamina predicted from the recording in the chiasm of Fig. 5C. From these comparisons (Fig. 5A with 5D and Fig. 5B with 5C) we conclude that both the measurements and the theoretical predictions are similar. The chiasm responses have a blunted peak and reduced noise. Both effects are readily explained by Fig. 5E, which shows the response predicted in the medulla terminal of the LMC to a short voltage pulse in the lamina. In essence, the axon and terminal form a low-pass filter, reducing the noise but also attenuating sharp transients. The effect of this noise suppression can be seen in Fig. 5F. Curve a shows the response of an LMC, measured in the lamina, to a sinusoidal modulation of light intensity at a frequency of 20 Hz. Curve b shows the predicted response at the medulla terminal. Note that the noise is strongly suppressed but the light response is reduced negligibly. Figure 5G summarizes the effect on signal and noise of transmission along the model LMC axon cable. Curve a shows the amplitude spectrum of the signal in a light-adapted LMC, obtained by taking the Fourier transform of a low amplitude impulse response to a flash of light (Laughlin et al. 1987). Curve b is the measured amplitude spectrum of LMC noise in the same light-adapted state (Laughlin et al. 1987), and curve c the filter properties of axon and terminal (amplitude of the transfer function for voltages – A_{tr}, see Appendix A – from lamina to medulla) derived from our model. These filter properties are such that most of the frequencies containing the signal are attenuated little or moderately, whereas higher frequencies, consisting mostly of noise not related to the stimulus, are attenuated more severely.

Discussion

We have derived a passive electrical model for the transmission of graded potentials through LMCs from lamina to medulla. The model successfully accounts for the cell's responses to current injection in both the synaptic zone of an LMC and its axon, and predicts the changes in response waveform and noise that occur during transmission. Our analysis allows us to address two questions. Firstly, to what extent are the membrane properties of LMCs adjusted to ensure that signals are transmitted efficiently between the neuropils of the lamina and the medulla? The second question is more general. What constraints determine the transmission properties of graded potential neurons and how much freedom do these limitations allow for designing a neuron with the desirable transmission and filter properties of LMCs? In other words, would it be possible to choose a different anatomical design of the neuron with different membrane parameters, while maintaining its performance?

Signal transfer between neuropils

We find that LMCs consist of a synaptic area of low impedance driving an axon and terminal of very high impedance. This is in substantial agreement with both the anatomical data and previous studies. The majority of measurements of fly LMC input resistance suggest that the synaptic zone has a much lower input resistance than the axon (Guy and Srinivasan 1988; Laughlin and Osorio 1989). The lower resistance correlates with the large number of photoreceptor synapses and these have been inferred to be tonically active in both darkness and steady light (Laughlin et al. 1987; Laughlin and Osorio 1989; Weckström et al. 1989). The large number of synapses has previously been regarded as a means of reducing the effects of synaptic noise (Laughlin 1973; Laughlin et al. 1987). Our model suggests a second and complementary role, the provision of sufficient current to drive the axon. The specific membrane resistance we infer for the axon, $>50 \cdot 10^5$ M$\Omega \cdot \mu m^2$, is at least 5 times the value previously derived from the maximum response amplitudes recorded at different locations in the chiasm (Zettler and Järvilehto 1973). Our estimate was made from charging curves recorded in the lamina. Consequently, the axon was not damaged by electrode penetration. Such high specific membrane resistances are not unprecedented in arthropod visual systems. Higher values ($196 \cdot 10^5$ M$\Omega \cdot \mu m^2$) have been estimated for the axons of barnacle photoreceptors, which transmit graded responses over several millimeters (Hudspeth et al. 1977).

The low input resistance of the synaptic zone and the high specific resistance of the axon play a critical role in signal transmission. The latter limits attenuation along the axon: a DC-signal is transmitted with an efficiency of close to 100%. The former ensures that the high frequencies contained in the photoreceptor signal are transmitted as well. Despite the high resistance of the axon membrane the system has a good frequency response because the charging and discharging of the axon and terminal are performed through the low impedance synaptic zone (van Hateren 1986). Thus, as in crayfish LMCs (Wang-Bennett and Glantz 1987), graded potential signals can be transmitted passively from lamina to medulla over distances of half a millimeter or more without boosting by active mechanisms. Such boosting mechanisms could potentially introduce spurious noise. Indeed, we find that one of the advantages of passive propagation is that, as first suggested by Shaw (1972), it provides a convenient low-pass filter for attenuating noise (Fig. 5G). It appears that the transmission properties of the cell are matched to the frequency components of the signal, and attenuate the noise generated at the input synapses in the lamina. Passive signal propagation brings with it two extra advantages. Firstly, we estimate that signals are transmitted from lamina to medulla within 1 ms, helping to keep the reaction time of the fly low. Second, with a low impedance synaptic zone at the peripheral end of the cell, signal transmission is fundamentally unidirectional (Wilson 1978; van Hateren

1986; Guy and Srinivasan 1988). This polarity has the advantage that local processing of LMC signals at the medulla terminals need have little effect on signal generation in the lamina. This conclusion is supported by the observation that a rapid component of the off transient is often prominent when recording close to the medulla but decreases in amplitude as one approaches the lamina, where it is rarely seen (Zettler and Järvilehto 1973; Guy and Srinivasan 1988).

The design of graded potential neurons

We can extend the conclusions derived from our cable model to study the roles played by the different anatomical and electrical parameters in determining signal transmission. To illustrate the trade-offs that can be made between different parameters, consider the adjustments that are required to compensate for the different axon lengths in the chiasm. LMCs from lateral parts of the lamina cross over to frontal parts of the medulla, and vice versa. The effect of this is a gradient of axon length across the eye, with shortest cells in the medial region. If we assume that the photoreceptors and synapses have temporal properties that do not vary with eye position – and there is no indication yet to the contrary – we might expect that the filter properties of the LMC should also be invariant, in order to maintain the selective suppression of noise. This invariance could be achieved in the face of a gradient of axon lengths by introducing compensatory gradients in other parameters.

As a measure of LMC filter properties we take the cutoff frequency f_c (the 3-dB point) of the voltage response in the medulla that results from current injected in the synaptic zone (R_{tr}, see Appendix A). If we increase the length of the axon, we will lower f_c. This can be compensated by adjusting one or several of the following parameters: f_c will increase by decreasing the specific membrane resistance of the synaptic zone, the capacitance of the terminal, the specific resistance of the axon membrane, the resistance of the terminal, or by increasing the diameter of the axon. In fact, gradients in several morphological parameters have been observed (Braitenberg and Hauser-Holschuh 1972; Hauser-Holschuh 1975; Strausfeld and Nässel 1981), but a systematic study of how all these parameters covary over the eye still lacks. We tentatively suggest that the variations might compensate for the effects of axon length on noise filtering. Given that LMCs vary in dimensions our model must be regarded as generic, in the sense that it describes the properties of a cell with average dimensions. Given adequate physiological and anatomical measurements the model can readily be modified to address the function of structural modifications, as demonstrated in the following section.

Our consideration of structural differences suggested that there are a number of possible interneuron designs, each capable of transmitting signals from one neuropil to another with the necessary frequency pass band. This possibility led us to investigate alternative ways of performing the same task, and to consider their relative merits. These evaluations suggest that some of the alternative designs are implemented in other types of neuron in the fly lamina.

Table 1. Comparison of 4 designs of neurons to transfer a signal from one neuropil to another. See text for details

	a	b	c	d
synaptic impedance	low	medium	medium	high
	20	60	60	
axon impedance	high	medium	high	active
	100	2.3	100	(spikes)
terminal impedance	high	high	medium	high
	inf.	inf.	80	inf.
efficiency	high	medium	medium	maximal
	0.99	0.69	0.59	1.0
unidirectionality	high	medium	low	maximal
	0.58	0.26	0.06	1.0
synaptic space	high	medium	medium	low
	5.0	1.7	1.7	
axon space	medium	medium	medium	low
	5.7	5.7	5.7	
metabolic cost	high	medium	medium	low
	5.0	2.8	2.4	
remarks		coupling		coding

Table 1 summarizes four neural designs that connect two neuropils via an axon of 400 μm. Designs a, b and c use graded potentials with different combinations of synaptic, axon and terminal impedance. Each design is evaluated by appropriate modification of the cable model. Parameters are selected to give an f_c (see above) of 130 Hz so that each design filters the signal and noise in an identical way. Design d uses spikes, and here the information transferred will depend strongly on the type of spike coding used, and the relationship between coding and photoreceptor signal and noise.

Table 1 also gives several measures of the performance of a neuron that could be important for the animal in terms of costs and benefits. Where possible we have used the model to estimate these costs and benefits, as indicated by the figures in the lower right corners of the appropriate boxes. Consider first the benefits. The most important is the efficiency of transfer of signal, here defined as the fraction of a DC-signal transferred along the axon. Note that this fraction represents the amplitudes of all other signal components because we have designed the neurons to have identical frequency responses. When the efficiency is low, the signals arriving at the terminal will have been attenuated to such an extent that they may not be able to trigger synaptic mechanisms efficiently and are bound to be corrupted by noise introduced along the axon and at the terminal.

A second characteristic which may be beneficial is unidirectionality, the property of transmitting signals well in one direction, but less well in the other. Though a certain degree of bidirectionality may be a useful property inside a neuropil where extensive processing is performed, we suggest that it could be a less desirable property for neurons connecting neuropils with distinct func-

tions. Unidirectionality is defined here as

$$u=(V_{tr,ortho}-V_{tr,anti})/(V_{tr,ortho}+V_{tr,anti}), \quad (1)$$

where V_{tr} is the voltage transfer efficiency in either the orthodromic or antidromic direction. Thus $u=1$ or $u=-1$ if the neuron is completely unidirectional, and $u=0$ if the neuron is completely bidirectional, i.e. if it transmits signals as easily in both directions.

Now consider the costs. An important factor must be the space occupied by the neurons. Insect neuropils tend to be tightly packed with neurons, and using unnecessarily large neurons seems undesirable. The space the synaptic zone needs depends on the membrane area required to get the correct synaptic impedance and includes the dendrites needed for making contact with the presynaptic neurons. To estimate the synaptic space we assumed that each synapse occupied a unit volume and contributed a unit conductance. Thus space is proportional to conductance, given a space factor that we define as 100/(synaptic impedance). The axon also occupies space, in proportion to its cross sectional area. In the examples of Table 1 we took the axon diameter as 2.7 μm for the graded potential neurons. Though not shown in the figure, similar arguments can be made about the space requirements of the terminal.

Finally, signal transmission requires metabolic energy because the ionic currents have to be balanced by pumping and each synaptic conductance channel must be activated by transmitter. Given that all model neurons have the same resting potential and produce the same range of response amplitudes in the synaptic zone, both the current and the amount of transmitter used will be proportional to conductance. Thus, as a rough estimate of metabolic cost, we took 100/(input resistance in the synaptic zone). The spiking neuron (d) will need less energy, because the amount of ions flowing during a spike is limited because of its short duration. Moreover, the diameter of the axon can be made much smaller, and thus the current needed for charging its membrane.

Now let us compare the different designs. Design a is the design we inferred for the LMCs. A low impedance synaptic zone drives a high impedance axon and terminal. The low impedance ensures the right frequency response of the neuron, gives good unidirectionality (see also van Hateren 1986), and it enables a high efficiency because it allows the axon and terminal to have a high impedance membrane. The drawbacks are increased space for the synaptic zone and a high metabolic cost.

For design b, the necessary frequency response is partly provided by the lower impedance of the axon. This decreases the space requirements of the synaptic zone, and to a lesser extent the metabolic cost, but it reduces the efficiency and unidirectionality. A further disadvantage of this design is that neurons whose axons run in parallel in tightly packed bundles can show considerable crosstalk (for example, it may be in the order of 10% for DC-signals in design b; see Appendix C).

In design c, the appropriate frequency response is produced by lowering the terminal impedance rather than the axon impedance. Compared with design b this has the advantage of avoiding crosstalk between neighbouring axons, but it has the disadvantage of having a very low unidirectionality. Compared with design a it occupies less space, and uses less energy but it is also much less efficient at transmitting signals.

Design d. Here the axon membrane supports spikes. In terms of space requirements, efficiency and unidirectionality this is the best design of the ones shown. The metabolic cost is harder to assess but it is unlikely to be as great as the simultaneous operation of 1200 chemical synapses, as implemented in a. However, the coding of signals with spikes is more complicated than with graded potentials. Measurements of the statistical efficiency of LMCs (De Ruyter and Laughlin, unpublished) suggest information transmission at rates in excess of 2000 bits/s, a figure that is supported by earlier measurements of signal and noise power spectra (Laughlin 1989). It is doubtful whether a comparable frequency response and information transfer rate can be reached with spikes, though this depends on the exact coding scheme used (see e.g. De Ruyter and Bialek 1988).

This comparison of design strategies shows that the fly has opted for the most expensive design (a), presumably because it provides the highest performance in graded potential coding. The justification for this expense is almost certainly the much higher metabolic cost of transduction. Under daylight conditions a fly photoreceptor achieves a signal to noise ratio of approximately 100:1, by having over 10000 transduction units active at any one time (Howard et al. 1987). As a result the cell is virtually short-circuited, with an input resistance of about 1–2 MΩ (Muijser 1979; Weckström and Laughlin, unpublished). Under constant illumination the LMC input resistance is close to the dark value of 15–20 MΩ because the synaptic input adapts (Laughlin and Osorio 1989). It follows that under daylight conditions the total energetic requirements of an LMC will be less than 10% of a photoreceptor's. Thus a modest expenditure in LMCs increases the amount of expensive receptor signal that is transmitted.

Cell types in the fly lamina

We can use our assessment of design principles to evaluate the relative performance of some of the different types of interneuron in the fly lamina, namely L1/L2, L3 and L4/5.

L1/L2 are the cells studied in this article. They have slightly different axon diameters (2.5 vs. 3.0 μm, Nicol and Meinertzhagen 1982) and differently shaped terminals, thus their transmitting properties may be slightly different. All else being equal, the smaller diameter of L1 will cause a cutoff frequency 10% lower than that of L2. This could be compensated for, however, by a 30% smaller membrane area of the terminal of L1 compared to that of L2 – assuming that the differences in the shapes of terminals can be neglected.

L3 has a synaptic membrane area which is less than one-third of the membrane area of L1/L2 (e.g. Strausfeld and Nässel 1981). Therefore, all else being equal, this cell is likely to have a higher impedance of the synaptic zone. Possibly L3 is designed as in Table 1 b or c, thus it could have a frequency response as good as that of L1/L2 at the expense of efficiency and unidirectionality. Given that L1 and L2 provide a more efficient input to the medulla, the value of this design is dubious. Another possibility is that L3 has an axon and terminal of high impedance and thus has a lower cutoff frequency than L1/L2. For example, if an L1/L2 had an axon of 400 μm length and a synaptic zone with a resistance of 20 MΩ, the cutoff frequency f_c would be 130 Hz, whereas a comparable L3 would have a synaptic zone with a resistance of 60 MΩ and an f_c of 84 Hz. Thus L3 could provide a low-pass filtered input to the medulla.

L4 and L5 are third order interneurons with very small synaptic zones, presumably giving a high resistance, and small diameter axons. Assuming a membrane area three times less than we assumed for L3, the resistance, all else being equal, would be 180 MΩ. Together with an axon diameter of 0.8 μm this leads to a cutoff frequency of 26 Hz. If L4 and L5 are using graded potentials as their means of signal propagation, they will not be able to transfer rapidly changing signals. It is more likely that L4 and L5 are using spikes (see e.g. discussions in Laughlin 1981; Shaw 1981), which is consistent with the small membrane area in the lamina and the small diameter of their axons.

Conclusion

We have derived a generic electrical model of the major graded potential neurons in the fly lamina, the LMCs. This model is based upon experimental data and predicts signal transmission properties that are similar to those observed. Our model also allows us to assess a number of design strategies for transmitting graded potential signals. The LMCs use the most expensive strategy with the highest performance, but the cost of transmission is small relative to that of phototransduction. If the neurons L3 are to transmit their graded signals to the medulla with relatively little decrement, then these signals will be strongly low-pass filtered. Our analysis has demonstrated that the geometry, synaptic drive and membrane properties of an LMC ensure the efficient passive propagation of the signal and the selective attenuation of synaptic noise. Both LMC morphology and synaptic density are rather precisely determined during development (rev. Meinertzhagen and Fröhlich 1983), and tend to be conserved during evolution (Strausfeld and Nässel 1981; Shaw 1989). This conservation may be explained, in part, by our finding that an LMC's structure promotes the efficient transmission of visual information.

Acknowledgements. We wish to thank N. Franceschini, R.C. Hardie, N.M. Jansonius, R. Menzel, D.G. Stavenga, and M. Weckström for valuable discussions and comments. This research was supported by the Committee for the Development of European Science and Technology (CODEST), by the Netherlands Organization of Scientific Research (NWO) to JHvH, and by the SERC to SBL.

Appendix A: Details of modelling and fitting

Units

The units we use are for length: μm; time: ms; frequency: kHz; voltage: mV; current: nA; resistance: MΩ; capacity: nF. These units are consistent, e.g. [ms] = [MΩ] × [nF] and [MΩ] = [mV]/[nA], and are 'natural units' for our purpose in the sense that they are often within a few orders of magnitude of values encountered when dealing with neurons, and are therefore routinely used by electrophysiologists.

Parameters

The parameters needed for the model are listed below. Clearly, there are too many parameters to use as free parameters in the fits. First, the fits would always look good with so many parameters, and second, the parameters could not be estimated accurately. The approach we took was to first estimate as accurately as possible those parameters known from the literature, and then try to get values for the remaining parameters from fits to the current injection measurements.

i_{in}: current injected through the microelectrode [nA].

C_{cb}: capacity of cell body, taken to be $260 \cdot 10^{-5}$ nF. This follows from the membrane area of a spherical cell body of 8 μm diameter plus a neck of 2 μm diameter and 10 μm length.

C_m: membrane capacity, taken to be 10^{-5} nF/μm², the standard literature value (e.g. Jack et al. 1975).

R_i: intracellular resistivity, taken to be 0.8 MΩ·μm. If the extracellular resistivity is not zero, it may be considered to be included in R_i; this would not change the calculations (see e.g. Jack et al. 1975, p. 27).

R_{mx}: specific membrane resistance of axon [MΩ·μm²], estimated from the fits.

R_{ms}: specific membrane resistance of synaptic zone [MΩ·μm²], estimated from the fits.

S_{ms}: membrane area per unit length of the synaptic zone, taken to be 18 μm²/μm, assuming a length of 50 μm for the synaptic zone. The resulting 900 μm² was obtained from estimates by Nicol and Meinertzhagen (1982; surface area of the stem of L1 and L2 300–370 μm², dendritic surface area 520–560 μm²). We are assuming here that our measurements were from either

L1 or L2. Occasionally we recorded from cells in the lamina with much larger resistances than the measurements presented in this article, and these cells may have been L3.

R_{ts}: total resistance of synaptic zone [MΩ], determined by R_{ms}, S_{ms}, and l_s.

S_{tt}: total membrane area of the terminal [μm²]. L1 and L2 are different, but we will use L2 as a reference. According to Strausfeld (1984, Fig. 7) the terminal consists of two branches of approximately 4 μm diameter and 15 μm length, resulting in an area of approximately 400 μm². Allowing for protuberance, we take S_{tt}= 1000 μm² as a rough estimate.

R_{tt}: total resistance of the terminal [MΩ], estimated from the fits.

a_s: radius of the synaptic zone, taken to be 1.35 μm (diameter 2.7 μm; according to Nicol and Meinertzhagen (1982) 2.5 μm for L1 and 3.0 μm for L2).

a_x: radius of the axon, taken to be 1.35 μm (diameter 2.7 μm).

l_s: length of the synaptic zone, taken to be 50 μm (e.g. Strausfeld 1976).

l_x: length of the axon [μm], estimated from the fits.

d_s: position of electrode in synapse (from cell body) [μm], assumed to be halfway.

d_x: position of electrode in axon (from the synapse) [μm], estimated from the fits.

The following parameters are properties of the neuron that we can determine from the model (for details and examples see van Hateren 1986).

R_{in}: input resistance (voltage at position 1 in response to a current injected at position 1).

R_{tr}: transfer resistance (voltage at position 2 in response to a current injected at position 1).

A_{tr}: voltage transfer (voltage at position 2 in response to a voltage imposed at position 1).

Several relationships between these parameters hold:

$$R_{ts} = R_{ms}/(S_{ms} \times l_s) \qquad (2)$$
$$A_{tr} = v_2/v_1 = (v_2/i_1)/(v_1/i_1) = R_{tr}/R_{in},$$

or

$$R_{tr} = R_{in} \times A_{tr}. \qquad (3)$$

Fitting procedures

The parameters that need to be determined from the fits are R_{mx}, R_{ms}, l_x and R_{tr} for measurements in the synaptic zone, and in addition to these d_x for measurements in the axon. Fitting with 4 or 5 parameters still does not yield very reliable estimates, therefore we decided to first fit the measurements from the synaptic zone while assuming R_{tr}=infinite, and then use the values so obtained for R_{mx} and R_{ms} for the fits to measurements in the axon. The assumption R_{tr}=infinite is not unreasonable for measurements in the lamina, because the terminal is relatively distant there. As free parameters for the synaptic zone fit we now have R_{ms}, R_{mx}, and l_x. For all measurements, the fits were the better the larger the value of R_{mx}. Values of $R_{mx} > 50 \cdot 10^5$ MΩ·μm² yielded fits already very similar to the limit of R_{mx}= infinite. We took $R_{mx} = 100 \cdot 10^5$ MΩ·μm² for the model calculations, but for these large values its exact value did not matter very much. Values obtained from the fits for l_x were consistent with independent estimates on the basis of the recording position of the electrode. We found $R_{ms} = 0.239 \pm 0.060 \cdot 10^5$ MΩ·μm² (see Table 2), $l_x = 413 \pm 118$ μm, and $R_{in} = 18.5 \pm 4.5$ MΩ; l_x is consistent with the known anatomical variation in axon length.

Table 2. Parameters obtained from fits of the responses of LMCs to current injected in two distinct regions, the synaptic zone in the lamina and the axon in the chiasm

Lamina recordings

Cell	i_{in} [nA]	R_{in} [MΩ]	R_{ms} [10^5 MΩ μm]	l_x [μm]
1	0.5	15.8	0.202	380
2	0.2	25.9	0.338	340
3	0.05	15.3	0.196	440
4	0.05	17.4	0.224	320
5	0.02	21.9	0.286	640
6	−0.02	14.7	0.188	360
Mean		18.5	0.239	413
st. dev.		4.5	0.060	118

Chiasm recordings

Cell	i_{in} [nA]	R_{in} [MΩ]	l_x [μm]	d_x [μm]
7	−0.2	25.1	470	30
7	−0.1	28.5	510	55
8	0.1	21.7	400	5
8	−0.1	22.3	400	10
9	−0.05	52.9	290	230
9	−0.05	61.9	300	295
10	0.02	30.3	790	70
11	0.05	41.8	280	150
12	0.02	28.6	350	50
13	−0.05	26.5	430	40
13	−0.05	30.7	350	70
14	−0.02	35.5	380	105
15	−0.02	29.8	580	65
Mean		33.5	425	
st. dev.		12.0	140	

Next, we fitted the measurements from the axons. In order to reduce the number of free parameters, we fixed $R_{ms}=0.25\cdot10^5$ MΩ·μm^2 and $R_{mx}=100\cdot10^5$ MΩ·μm^2 (the values we determined from the lamina fits), and we used l_x, d_x and R_{tr} as free parameters. For all measurements the fits were best for very large R_{tr}, thus R_{tr} is infinite for practical purposes. This justifies our original assumption, made when fitting the measurements in the synaptic zone. We found $l_x=425\pm140$ μm and $R_{in}=33.5\pm12.0$ MΩ (see Table 2, R_{in} varying between 21.7 and 61.9 MΩ, depending on the distance of the electrode from the lamina). The value of l_x is consistent with what we determined from measurements in the synaptic zone, an indication of the reliability and consistency of the model.

Appendix B: The role of the dendrites of LMCs

Each LMC has about 180 dendrites (Nicol and Meinertzhagen 1982), for which we assume an average length of 3 μm and an average diameter of 0.125 μm. This leads to a total axial series resistance $R_{ser}=3\times0.8/(\pi\times0.0625^2)=196$ MΩ. If the specific membrane resistance is $0.25\cdot10^5$ MΩ·μm^2 (see Appendix A), and if we consider the dendrite as a cable, its space constant $\lambda=31$ μm. Thus the space constant of a dendrite is much larger than its length. Therefore, the dendrite will be isopotential to a good approximation, unless the resistance R_{syn} at its far end (i.e., at the synapse) is similar to or smaller than R_{ser} (in that case R_{syn} would provide a low-resistance pathway to ground and produce a voltage drop over R_{ser}, as recently suggested for retinal horizontal cells, Winslow et al. 1989). This is in general not the case in LMCs, because in contrast to vertebrate horizontal cells LMCs have a higher resistance during steady illumination than during a response to an intensity increment (Laughlin and Osorio 1989). If we assume that all conductances are situated in the dendrites, then each of the 180 dendrites must have a resistance $R_d=20\times180=3600$ MΩ, assuming an input resistance of 20 MΩ for the LMC (as seen from its main stem). Thus R_{syn} must be much larger than R_{ser} (=196 MΩ), because $R_d=R_{ser}+R_{syn}$ (neglecting the contribution of nonsynaptic membrane of the dendrite). Only when the resistance of the LMC drops to low values during saturating light responses will isopotentiality break down. For example, if the LMC resistance drops to 2 MΩ, the resistance of each dendrite is 360 MΩ and R_{syn} approaches R_{ser}. Thus the series resistance of the dendrites is unlikely to limit current flow in LMCs, unless during saturating responses. The properties of the dendrites have to be considered if one aims at understanding saturating responses as in Fig. 5A and C in terms of the underlying synaptic currents. They do not influence the voltage transfer shown in Fig. 5, however, because the voltage response recorded in the lamina already accounts for the currents required to drive the axon and terminal; i.e. the properties of the synaptic zone do not enter the equations for calculating the voltage transfer A_{tr} (van Hateren 1986).

Appendix C: Coupling between neighbouring axons

The signal propagation through two identical, half-infinite cables, coupled through a non-zero extracellular resistivity is described by a system of two coupled differential equations. If one of these cables is stimulated, while the other is left undisturbed, there will be crossover of the signal from the stimulated to the unstimulated. In the frequency domain we define the coupling c as the ratio, per frequency, of the amplitude of the signal in the unstimulated and the stimulated cable. Solving the coupled differential equations with the appropriate boundary conditions yields

$$c(x)=(\exp(-x/l_1)-\exp(-x/l_2))/\exp(-x/l_1)+\exp(-x/l_2)), \quad (4)$$

where x is the distance from the beginning of the cables, and

$$l_1=(z_m/z_i)^{\frac{1}{2}} \quad (5)$$

$$l_2=(z_m/(z_i+2z_e))^{\frac{1}{2}}, \quad (6)$$

with z_m the impedance of the membrane per unit length cable (see Fig. 1), $z_i=r_i$ the intracellular resistance per unit length cable, and $z_e=r_e$ the extracellular resistance per unit length cable.

References

Braitenberg V, Hauser-Holschuh H (1972) Patterns of projection in the visual system of the fly. II. Quantitative aspects of second order neurons in relation to models of movement perception. Exp Brain Res 16:184–209

Guy RG, Srinivasan MV (1988) Integrative properties of second-order visual neurons: a study of large monopolar cells in the dronefly *Eristalis*. J Comp Physiol A 162:317–331

Hateren JH van (1986) An efficient algorithm for cable theory, applied to blowfly photoreceptor cells and LMC's. Biol Cybern 54:301–311

Hateren JH van (1987) Neural superposition and oscillations in the eye of the blowfly. J Comp Physiol A 161:849–855

Hauser-Holschuh H (1975) Vergleichende quantitative Untersuchungen an den Sehganglien der Fliegen *Musca domestica* und *Drosophila melanogaster*. Doctoral Dissertation, Eberhard-Karls-Universität, Tübingen

Howard J, Blakeslee B, Laughlin SB (1987) The intracellular pupil mechanism and photoreceptor signal:noise ratios in the fly *Lucilia cuprina*. Proc R Soc Lond B 231:415–435

Hudspeth AJ, Poo MM, Stuart AE (1977) Passive signal propagation and membrane properties in median photoreceptors of the giant barnacle. J Physiol (Lond) 272:25–43

Jack JJB, Noble D, Tsien RW (1975) Electric current flow in excitable cells. Clarendon Press, Oxford

Järvilehto M, Zettler F (1971) Localized intracellular potentials from pre- and postsynaptic components in the external plexiform layer of an insect retina. Z Vergl Physiol 75:422–440

Laughlin SB (1973) Neural integration in the first optic neuropile of dragonflies. I. Signal amplification in dark-adapted second order neurons. J Comp Physiol 84:335–355

Laughlin SB (1981) Neural principles in the visual system. In: Autrum H (ed) Vision in invertebrates (Handbook of sensory physiology, vol VII/6B). Springer, Berlin Heidelberg New York, pp 133–280

Laughlin SB (1987) Form and function in retinal processing. Trends Neurosci 10:478–483

Laughlin SB (1989) The reliability of single neurons and circuit design – a case study. In: Durbin R, Miall RC, Mitchison G (eds) The computing neuron. Addison-Wesley, New York, pp 322–336

Laughlin SB, Hardie RC (1978) Common strategies for light adaptation in the peripheral visual systems of fly and dragonfly. J Comp Physiol 128:319–340

Laughlin SB, Osorio D (1989) Mechanisms for neural signal enhancement in the blowfly compound eye. J Exp Biol 144:113–146

Laughlin SB, Howard J, Blakeslee B (1987) Synaptic limitations to contrast coding in the retina of the blowfly *Calliphora*. Proc R Soc Lond B 231:437–467

Meinertzhagen IA, Fröhlich A (1983) The regulation of synapse formation in the fly's visual system. Trends Neurosci 6:223–228

Muijser H (1979) The receptor potential of retinular cells of the blowfly *Calliphora*: the role of sodium, potassium and calcium ions. J Comp Physiol 132:87–95

Nicol D, Meinertzhagen IA (1982) Regulation in the number of fly photoreceptor synapses: The effects of alterations in the number of presynaptic cells. J Comp Neurol 207:45–60

Ruyter van Steveninck RR de, Bialek W (1988) Real-time performance of a movement-sensitive neuron in the blowfly visual system: coding and information transfer in short spike sequences. Proc R Soc Lond B 234:379–414

Segev I, Fleshman JW, Miller JP, Bunow B (1985) Modelling the electrical behavior of anatomically complex neurons using a network analysis program: passive membrane. Biol Cybern 53:27–40

Shaw SR (1972) Decremental conduction of the visual signal in the barnacle lateral eye. J Physiol (Lond) 220:145–175

Shaw SR (1981) Anatomy and physiology of identified non-spiking cells in the photoreceptor-lamina complex of the compound eye of insects, especially Diptera. In: Roberts A, Bush BMH (eds) Neurons without impulses. Cambridge University Press, Cambridge, pp 61–116

Shaw SR (1984) Early visual processing in insects. J Exp Biol 112:225–251

Shaw SR (1989) The retina-lamina pathway in insects, particularly Diptera, viewed from an evolutionary perspective. In: Stavenga DG, Hardie RC (eds) Facets of vision. Springer, Berlin Heidelberg New York, pp 186–212

Strausfeld NJ (1976) Atlas of an insect brain. Springer, Berlin Heidelberg New York

Strausfeld NJ (1984) Functional neuroanatomy of the blowfly's visual system. In: Ali MA (ed) Photoreception and vision in invertebrates. Plenum Press, New York London, pp 483–522

Strausfeld NJ, Nässel DR (1981) Neuroarchitecture of brain regions that subserve the compound eyes of Crustacea and insects. In: Autrum H (ed) Vision in invertebrates (Handbook of sensory physiology, vol VII/6B). Springer, Berlin Heidelberg New York, pp 1–132

Wang-Bennett LT, Glantz RM (1987) The functional organization of the crayfish lamina ganglionaris. I. Nonspiking monopolar cells. J Comp Physiol A 161:131–145

Weckström M, Kouvalainen E, Djupsund K, Järvilehto M (1989) More than one type of conductance is activated during responses of blowfly monopolar neurons. J Exp Biol 144:147–154

Wilson M (1978) Generation of graded potential signals in the second order cells of locust ocellus. J Comp Physiol 124:317–331

Winslow RL, Miller RF, Ogden TE (1989) Functional role of spines in the retinal horizontal cell network. Proc Natl Acad Sci USA 86:387–391

Zettler F, Järvilehto M (1973) Active and passive axonal propagation of non-spike signals in the retina of *Calliphora*. J Comp Physiol 85:89–104